Macromolecules

Article

Cite This: *Macromolecules* 2018, 51, 8205−8216

pubs.acs.org/Macromolecules

Use of pH Gradients in Responsive Polymer Hydrogels for the Separation and Localization of Proteins from Binary Mixtures

Annika Hagemann, Juan M. Giussi, and Gabriel S. Longo*

Instituto de Investigaciones Fisicoquímicas Teóricas y Aplicadas (INIFTA), UNLP-CONICET, La Plata, Argentina

Supporting Information

ABSTRACT: Using a molecular-level equilibrium theory where proteins are described using their crystallographic structure, we have studied protein adsorption from binary and ternary mixtures of myoglobin, lysozyme, and cytochrome *c* to poly(methacrylic acid) hydrogel films. The pH gradients these films induce can lead to selective protein adsorption, where the solution pH provides a sensible dial to externally control protein separation. Changing the chemical composition of the polymer network, adding either another acidic or a neutral comonomer, allows for protein localization to controlled spatial regions of the film with nanometer resolution. As pH-sensitive polymer hydrogels are promising candidates for smart, responsive biomaterials, understanding the complexity of competitive protein adsorption is essential. In this work, we highlight the decisive role of amino acid protonation in selective protein adsorption. We present conditions such that the hydrogel film will selectively incorporate the more weakly charged protein, provided that it requires less work to protonate its amino acids.

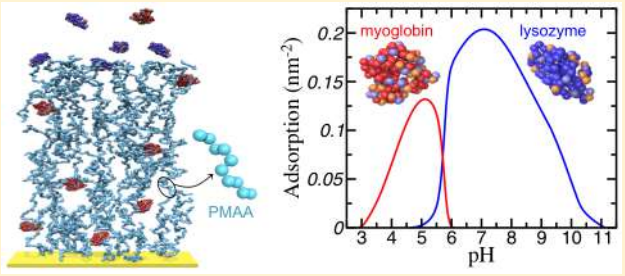

INTRODUCTION

Because of their highly tunable properties and biocompatibility, polymer hydrogels have been of great interest as materials for biomedical applications. In oral drug delivery, these hydrogels have been intensely investigated as carriers that can encapsulate and deliver protein drugs, protecting them through the physical and chemical barrier that the gastrointestinal environment imposes.[1] Within the aqueous tissue-like microenvironment inside the cross-linked polymer network, proteins are less susceptible to denaturation and aggregation.[2,3] Moreover, proteins retain their structure and activity when delivered from polymer hydrogels.[4] Besides drug delivery, polymer hydrogels have great interest as the responsive component in many other biomedical applications[5,6] including tissue engineering,[7] biosensing,[8,9] and the design of functional biomimetic materials.[10]

The use of hydrogels or any other material in biomedical devices requires a deep understanding of its interaction with proteins. For example, contact lenses based on gels of poly(methacrylic acid) (PMAA) adsorb proteins from tear liquid, which has implications for wear comfort and the occurrence of inflammatory complications.[11,12] However, selective adsorption of proteins with antibacterial and/or anti-inflammatory properties, such as lysozyme, might be beneficial in this and other contexts.[12] When applied in biological environments, the gel is exposed to multicomponent mixtures, and the adsorption of proteins to the material is governed by a complex interplay between the polymer network and the different molecular species present in the environment. The presence of other proteins or biomolecules can influence protein adsorption in a nontrivial way; the adsorption from protein mixtures cannot be predicted from the behavior of single protein solutions.[13] Thus, understanding the physical chemistry that governs protein adsorption from mixtures is essential.

In this work, we present a step forward into that direction and apply a molecular theory to investigate the equilibrium conditions of competitive adsorption from binary and ternary protein mixtures to pH-responsive hydrogel films. Our approach allows for a molecular-level description of the size, shape, charge distribution, and conformational degrees of freedom of all components of the system, including the different proteins and the polymer network that makes the backbone of the film. A less general version of this theory has been recently used to describe His-tag and lysozyme adsorption to polyacid hydrogel films.[14,15] These previous studies highlight the critical and nontrivial role of amino acid protonation to favor protein adsorption[16] as well as the significance of pH and ionic strength in controlling adsorption. Here we show that, in addition to the expected and important role of the charge of the protein, amino acid protonation is a decisive factor to determine selective adsorption.

Protein adsorption to pH-sensitive polymeric materials has been subject of different experimental studies. Using isothermal calorimetry, Welsch et al.[17] considered lysozyme adsorption to core−shell microgels based on poly(acrylic acid)

Received: August 30, 2018
Revised: October 1, 2018
Published: October 9, 2018

DOI: 10.1021/acs.macromol.8b01876
Macromolecules 2018, 51, 8205−8216

(PAA) units. In agreement with the aforementioned theoretical studies, this work highlights the important role of protein protonation upon adsorption to the microgel. Moreover, Zhang et al.[18] studied the influence of pH on the kinetics of adsorption and release of whey proteins from alginate-based hydrogel beads. Competitive adsorption of proteins to a variety of surfaces, from hydrophilic to having different degrees of hydrophobicity, has also been studied using several different experimental techniques.[13,19−21] Recently, Moerz and Huber[22] studied the adsorption of cytochrome *c*, myoglobin, and lysozyme in mesoporous thin films to propose that these materials can be applied for protein separation in binary mixtures by means of adjusting the solution pH. In such study, changing the pH allowed for effective separation of myoglobin and lysozyme; one protein can prevent adsorption of the other, even when this latter would strongly adsorb from pure solutions.[22] Saxena et al.[23] prepared positively and negatively charged organic−inorganic hybrid membranes to show protein separation in lysozyme and bovine serum albumin mixtures depending on the sign of membrane charge and the pH.

In addition to these experimental studies, various theoretical and simulation studies have been conducted on protein adsorption. By use of molecular dynamics (MD) simulations, single protein adsorption to different surfaces[24,25] and to nanoparticles[26−29] have been extensively investigated. Based on the same technique, competitive binding of proteins to gold nanoparticles has been considered.[30] Furthermore, the interaction between charged polymers in solution and proteins has been the subject of theoretical and molecular simulations studies.[31,32] However, protein adsorption to polymeric materials or polymer-modified surfaces has been less frequently considered. Yigit et al.[33] developed different Langmuir binding models to investigate lysozyme adsorption to core−shell microgels, where the state of charge of the microgels can be modified by the adsorbate. Angioletti-Uberti et al.[34] developed a dynamic density functional theory approach to describe lysozyme adsorption on charged, polymer-coated nanoparticles. Sun et al.[35] performed MD simulations at different pH values of the adsorption and complexation of the fragment antigen-binding of trastuzumab to a poly(vinyl alcohol) hydrogel. Szleifer and co-workers developed a molecular theory to investigate protein adsorption on grafted polymer layers.[36,37] With regard to competitive adsorption, we can only mention the multicomponent cooperative binding model developed by Oberle et al.[38] to investigate competitive adsorption of proteins to a soft polymeric layer.

In this work we investigate competitive protein adsorption to polyacid hydrogel films. We focus our attention on a poly(methacrylic acid) network, but we also consider networks having another acidic polymer or a neutral polymer. Our goal is to show that these films can be used to separate and localize proteins with nanometric spatial precision. The chemical composition of the network can be modified to prevent or enhance selective adsorption to different regions inside film or to the film−solution interface. Moreover, solution pH provides a sensible dial to externally control such separation and localization. As model proteins, we study mixtures of similar-sized globular proteins, using myoglobin (16.7 kDa), lysozyme (14.4 kDa), and cytochrome *c* (12.4 kDa). On the basis of our theoretical study, we analyze the main physicochemical factors driving selective protein adsorption from these mixtures under different environmental conditions.

METHODS

Theoretical Approach. To investigate the thermodynamics of competitive protein adsorption to PMAA films, we resource to a theory that allows for a molecular-level description of all the components including the different proteins and the polymer network. This molecular description accounts for size, shape, charge distribution, and conformational degrees of freedom of each species. In this theory, the protonation states of protein amino acids and network segments are not assumed *a priori* as a result of the solution (bulk) pH; rather, they are predicted depending on the group position and its local environment. In other words, at each position the chemical state of a molecule results from the local interplay between the free energy cost of protonation/deprotonation, the entropic loss of molecular confinement, the conformational degrees of freedom of the network and the proteins, and the electrostatic, van der Waals, and steric interactions. This is achieved through the formulation of a general free energy that includes all these contributions. A simpler version of this molecular theory was recently developed to describe adsorption of histidine peptides to grafted polyacid networks and later extended to consider lysozyme adsorption in such films.[14,15] The method represents an extension of approach used by Nap et al.[39] and Gong et al.[40] to investigate the behavior of grafted weak polyelectrolyte layers. In this present work, we generalize the theoretical framework to investigate the adsorption to pH-responsive films from solutions containing different proteins (or other molecules). Next, we present the main characteristics of the method while more details and explicit expressions can be found in the Supporting Information.

The system of study consists of an aqueous solution in contact with a poly(methacrylic acid) network that is chemically grafted to a planar surface (see Figure 1). Coordinate z gives the distance from the surface that sits a $z = 0$. The solution contains water molecules (w), hydronium (H_3O^+), and hydroxide (OH^-) ions and a monovalent salt (NaCl) dissociated into chloride (Cl^-) and sodium (Na^+) ions. In addition, this solution can contain any number of different species of proteins in finite concentrations. In particular, we consider pure, binary, and ternary solutions of myoglobin (myo), lysozyme (lyso), and cytochrome *c* (cyto). We have chosen these proteins because they are three globular proteins with similar size (1.5 nm diameter), typically considered in experimental studies.

The first step in this research method consists in writing the total (Helmholtz) free energy of the system:

$$F = -TS_{\mathrm{cnf,nw}} + F_{\mathrm{chm,nw}} - TS_{\mathrm{mix}} + \sum_i (-TS_{\mathrm{cnf},i} - TS_{\mathrm{tr},i} + F_{\mathrm{chm},i}) + U_{\mathrm{st}} + U_{\mathrm{vdw}} + U_{\mathrm{elect}} \quad (1)$$

where T is the temperature and the subindex i runs over all the species of proteins that are present in the solution. The first term on the right-hand side of this equation is associated with the conformational entropy of the network ($S_{\mathrm{cnf,nw}}$), arising from the many different molecular conformations that the cross-linked polymeric structure can assume. By conformation we denote a particular spatial distribution of all the MAA segments. The second term is the chemical free energy of the network ($F_{\mathrm{chm,nw}}$) that describes the acid−base equilibrium of its ionizable segments. The next term accounts for the translational (mixing) entropy of all free species (S_{mix}), except proteins, as well as the formation self-energies of these species. The next sum runs over all the proteins that are present in the mixture; for a particular protein (i), these terms include its conformational entropy ($S_{\mathrm{cnf},i}$), its translational entropy and self-energy ($S_{\mathrm{tr},i}$), and the chemical free energy ($F_{\mathrm{chm},i}$) that describes the acid−base equilibrium of its titratable amino acids. Finally, the energetic contributions include steric, excluded volume repulsions (U_{st}), van der Waals attractions (U_{vdw}), and electrostatic interactions (U_{elect}).

Each of these free energy contributions can be expressed as a functional of the following quantities: (1) the probability distribution of network conformations, (2) the local densities of all free species,

DOI: 10.1021/acs.macromol.8b01876
Macromolecules 2018, 51, 8205−8216

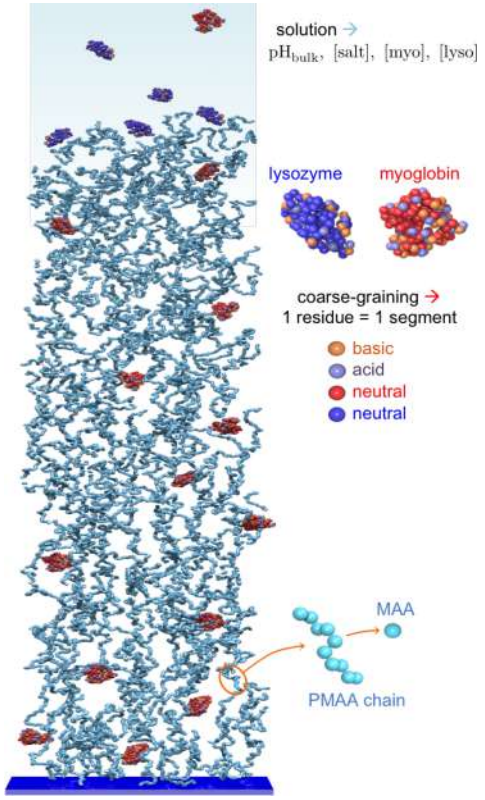

Figure 1. Scheme representing the system of study. A binary mixture of proteins (myoglobin and lysozyme) in an aqueous solution is in contact with a network of cross-linked PMAA chains grafted to a planar surface. Far from network, the (bulk) solution composition is controlled, including its pH, salt, and protein concentration. The scheme illustrates experimental conditions such that myoglobin adsorbs inside the network while lysozyme adsorbs at the top surface of the polymer film. In our molecular model, each amino acid residue is represented by a single coarse-grained particle that can be either electroneutral or titratable (neutral units are represented in different colors for each protein). Similarly, each PMAA segment is described by a single particle bearing an acid group.

including those of (different conformations of) the proteins, (3) the local degrees of protonation of all titratable species including those of network segments and protein amino acids, and (4) the local electrostatic potential. Under the conditions of our study, the thermodynamic potential that describes the equilibrium of this system is the semigrand potential (Ω), which is the Legendre transform of the Helmholtz free energy (eq 1). This thermodynamic potential is a function of the chemical potentials of all the free species, which are fixed due to the chemical equilibrium with the bath solution. Optimizing Ω with respect to the aforementioned functions allows for expressing such quantities in terms of only two position-dependent interaction potentials: the local osmotic pressure and the electrostatic potential. Therefore, the total free energy functional (and each of its contributions) can be expressed in terms of these two interaction potentials; this makes explicit the coupling that exists between chemical state, molecular organization, conformational degrees of freedom, physical interactions, and local environment.

These local interaction potentials can be obtained through the numerical solution of both the Poisson equation and the incompressibility constraint imposed to the fluid system. This last constraint assures that at each position the volume is completely occupied by some of the molecular species (see the Supporting Information). Once these interaction potentials are determined, the free energy is known, and thus any thermodynamic quantity of interest can be calculated. In addition, the local functions that compose the free energy are all known as well, which allows for the calculation of different local quantities.

Molecular Model. To apply this theory, a molecular model must be defined to describe all chemical species that compose the system. In particular, the set of molecular conformations of the polymer network is an input of the method. This network is composed of cross-linked 50-segment long polymer chains, where each segment is a coarse-grained representation of a MAA unit. The volume of a MAA segment is 0.085 nm^3, its acid dissociation constant is given by pK_{MAA} = 4.65, and the segment length is 0.5 nm. Most of these chains connect two cross-linking segments, except those topmost chains, which have their solution-side ends free, and some chains that are connected by one of their ends to a surface-grafted segment. Cross-linking units are 4-coordinated, and the structure has diamond-like topology.[41−44] To generate network conformations, we have performed MD simulations using GROMACS 5.1.2.[45−47] In these MD simulations, the network is a periodic molecule composed of 30 cross-linking segments, 2 grafting points, and 64 chains with 3200 MAA units in total. The area of the supporting surface in the MD simulation box is A = 40.3 nm^2, and periodic boundary conditions are imposed in the x and y directions. The force field used in the MD simulations has been well described in other works.[41,43,48,49]

Proteins are represented using a coarse-grained model where all the atoms of an amino acid are described by a single particle centered at the position of the corresponding α-carbon (see Figure 1).[15,51] The volume of these coarse-grained units is 0.135 nm^3. Sequence and position of all α-carbons are taken from the protein crystallographic structure PDB file (3RGK, 193L, and 2B4Z for myoglobin,[52] lysozyme,[53] and cytochrome c,[54] respectively). The positions of all residues are kept fixed with respect to the protein center of mass according to its original crystallographic structure, independently of the pH. The proteins, however, have rotational and translational freedom. We have considered solutions where the concentration of a given protein is 10 μM, if the species is in the solution. Amino acids are divided in two groups: neutral and titratable. The latter group includes the acidic units, aspartic acid (Asp), glutamic acid (Glu), and tyrosine (Tyr), as well as the basic units, which are arginine (Arg), histidine (His), and lysine (Lys). The heme complex with two acid groups is modeled as two titratable coarse-grained units and the pK_a of the C- and N-terminal groups considered. Other amino acids are considered charge neutral. Table 1 shows the pK_a values used for the titratable amino acids as well as the number of each residue type in the proteins (composition number).

Using the pK_a scheme of Table 1, Figure 2 shows the charge of each protein in dilute solution as a function of pH. Looking at these

Table 1. pK_a Values of the Coarse-Grained Units Used in Our Molecular Model[a]

	Asp	Glu	Tyr	Arg	His	Lys	Nt	Ct	heme	neu
pK_a	3.5	4.2	10.3	12.0	6.6	10.5	7.7	3.3	3.8	
N_{myo}	8	14	2	3	9	19	1	1	2	94
N_{lyso}	7	2	3	11	1	6	1	1		99
N_{cyto}	3	6	5	1	3	18	1	1	2	68

[a]These values are taken from Grimsley et al.[50] and correspond to average values over different proteins obtained from several experimental results. For cytochrome c, we have used its experimental results of pK_a = 2.4, 2.9,and 6.35 for its three histidine residues, as they vary significantly from the average value. Nt and Ct (terminal) are not additional coarse-grained units, but they add a titratable group to the terminal residues.

DOI: 10.1021/acs.macromol.8b01876
Macromolecules 2018, 51, 8205−8216

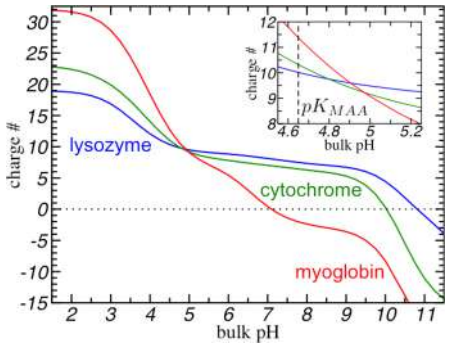

Figure 2. Plot showing the net charge of the three proteins of interest in dilute solution as a function of the pH. The inset zooms in the intersections between these curves, which occurs near the pK_a of MAA (dashed vertical line).

curves already tells us to expect nonmonotonic adsorption to the PMAA film as a function of the pH, given that this behavior is driven by the electrostatic attractions between the oppositely charged network and proteins. At low pH, the proteins are strongly positively charged but the polymer network is not (pK_{MAA} = 4.65). Similarly at high pH, PMAA is charged, but the proteins have little positive or even negative charge. Only for intermediate pH, when both adsorbent and adsorbate are strongly charged with opposite sign, we anticipate adsorption to take place. Moreover, we note that the net charges of the proteins intersect each other when pH is around the pK_a of methacrylic acid (see the inset in Figure 2). Thus, we expect mixtures of these proteins to display interesting behavior around pH 5. This is an additional reason for our choice of proteins and polymer in this study.

Other inputs of our molecular model are the volume (and charge) of the rest of the free species: for water molecules as well as hydronium and hydroxide ions we use 0.03 nm^3, while the volume of sodium and chloride ions is 0.033 nm^3. To numerically solve the equations resulting from the molecular theory, the space is discretized into 0.5 nm thick layers parallel to the supporting surface (the x–y plane). The system is assumed to be isotropic in the x and y directions. The aqueous medium has dielectric constant $\epsilon = \epsilon_w\epsilon_0$, with ϵ_w = 78.5 being the relative dielectric constant of water at room temperature and ϵ_0 denoting the vacuum permittivity.

RESULTS

To quantify the partition of proteins inside the hydrogel film, we define the adsorption as the number of proteins adsorbed per unit area, in excess of the bulk contribution:

$$\Gamma_i = \int_0^\infty dz(\langle\rho_i(z)\rangle - \rho_i^{bulk}) \quad (2)$$

where $i \in$ {lysozyme, myoglobin, cytochrome} refers to the protein in question, having local and bulk concentration $\langle\rho_i(z)\rangle$ and ρ_i^{bulk}, respectively. Note that $\lim_{z\to\infty}\langle\rho_i(z)\rangle = \rho_i^{bulk}$.

Inspired by the findings of Moerz and Huber[22] showing selective adsorption of myoglobin or lysozyme to mesoporous silica depending on the pH, we first describe the behavior of solutions of these proteins. Figure 3 shows the adsorption of both proteins from binary mixtures with 1 mM (panel A) and 10 mM (panel B) salt concentration as well as the adsorption from single-protein solutions at the same conditions. Myoglobin adsorbs preferentially at lower pH values while lysozyme does in the higher pH range, which suggests that a polyacid network can serve as a tunable system for separation of the two proteins through varying the solution pH. These results are consistent with the relation between protein net charge and pH in the bulk solution, seen in Figure 2;

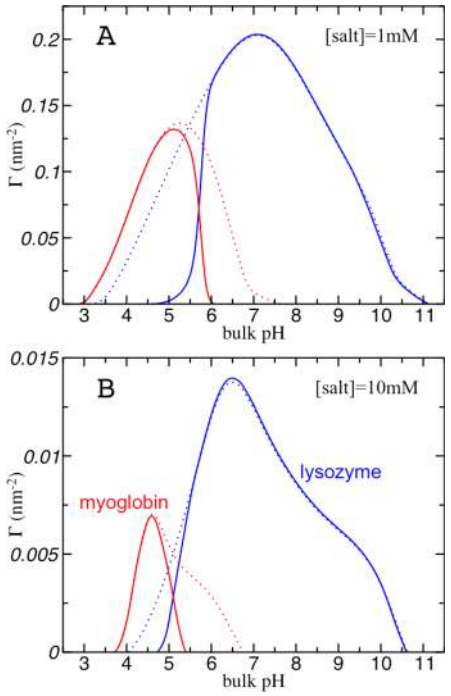

Figure 3. Protein adsorption, Γ_i, from myoglobin–lysozyme solutions with 1 mM (A) and 10 mM (B) salt concentration. Protein concentrations are [myo] = [lyso] = 10 μM. Dotted-line curves show the adsorption from single-protein solutions otherwise under the same conditions.

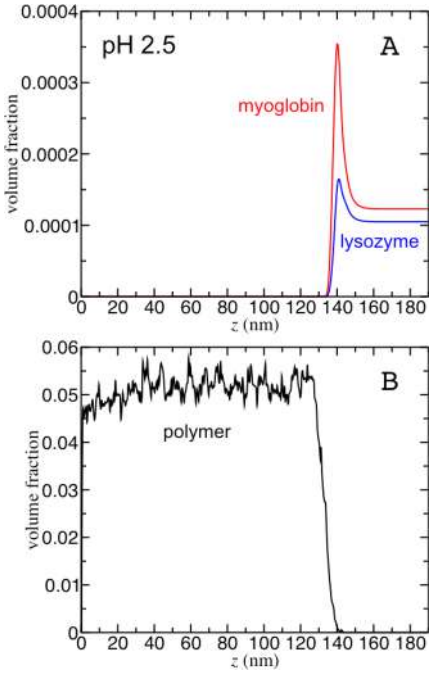

Figure 4. Volume fraction of the proteins (A) and polymer (B) as a function of the distance from the supporting surface (z = 0). The bulk solution pH is 2.5, [salt] = 1 mM, and [myo] = [lyso] = 10 μM.

myoglobin is more positively charged than lysozyme at low pH (bulk pH $\lesssim$ 5), while at higher values (bulk pH $\gtrsim$ 5), lysozyme has a more positive net charge. Moreover, solution myoglobin becomes negatively charged around bulk pH 7.

Compared to single-protein solutions, both the magnitude and the pH of maximum adsorption are not significantly

DOI: 10.1021/acs.macromol.8b01876
Macromolecules 2018, 51, 8205–8216

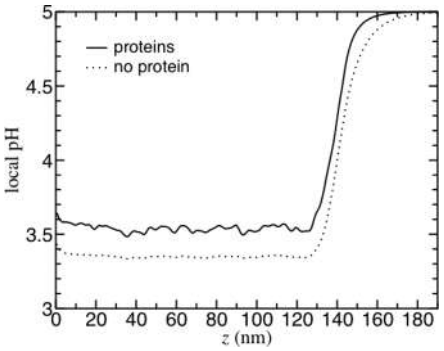

Figure 5. Plot of the local pH as a function of the distance from the supporting surface. Solid-line curve corresponds to a myoglobin–lysozyme solution ([myo] = [lyso] = 10 μM), while the dotted-line curve represents a salt solution with no proteins. In both systems, the bulk pH is 5 and the salt concentration is 1 mM.

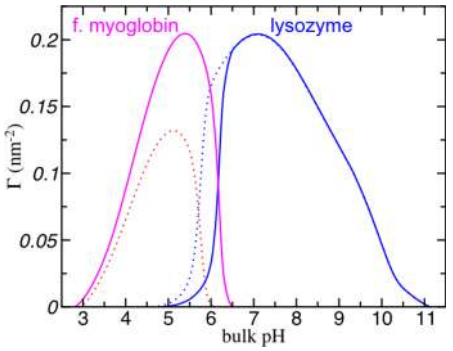

Figure 7. Plot of the pH-dependent protein adsorption from f. myoglogin–lysozyme solutions (solid-line curves). The graph also shows the adsorption from actual myoglobin–lysozyme solutions at the same conditions (dotted-line curves); [salt] = 1 mM, and the concentration of each protein is 10 μM.

affected by the presence of the other protein in binary mixtures. Depending on the salt concentration, adsorption peaks around pH 4.5 or 5 for myoglobin and pH 6.5 or 7 for lysozyme (see Figure 3). However, the range of pH where a particular protein adsorbs from binary mixtures shortens with respect to single-protein solutions. For example, for [salt] = 1 mM solutions, myoglobin completely prevents the adsorption of lysozyme in the range pH 3.5–5, which does occur in pure lysozyme solutions (see Figure 3A). At the same time lysozyme inhibits myoglobin adsorption in the range pH 6–7.5.

Decreasing the salt concentration enhances adsorption of both proteins from binary mixtures and single-protein solutions. In the cases shown in Figure 3, a 10-fold decrease in the salt concentration results in an order of magnitude increase in adsorption. At high salt concentration, both sodium and chloride ions adsorb inside the polymer network (see the Supporting Information), which results in the screening of network–protein electrostatic interactions that effectively become shorter range. At low salt concentration, confining ions inside the film becomes more entropically costly. Only enough counterions are confined to make the film electroneutral. Thus, the screening effect is less important, and protein–network interactions result effectively longer range. However, we note that the polymer network is significantly less charged at same pH when the salt concentration decreases (see Supporting Information), which indicates that the weaker charged network is capable of adsorbing more protein. This behavior highlights the importance of salt concentration and its screening effect over the role of the net amount of charge.

At low salt concentration, counterion release can significantly influence protein adsorption in confined environments.[55,56] Moerz and Huber[56] have shown that there are conditions where the release of counterions represents an important contribution to the binding of cytochrome *c* to mesoporous silica. Our theory can properly describe the entropy gain of ion release from the hydrogel film upon protein adsorption. At 10 mM salt, the concentration of sodium ions inside the film is roughly the same for both protein solutions and salt solutions without proteins (see the Supporting Information). Counterion release from the polymer network does not play a significant role under these conditions. At 1 mM salt, however, these concentrations can be significantly different from each other, particularly between pH 3 and 7 (see the Supporting Information), where protein adsorption can

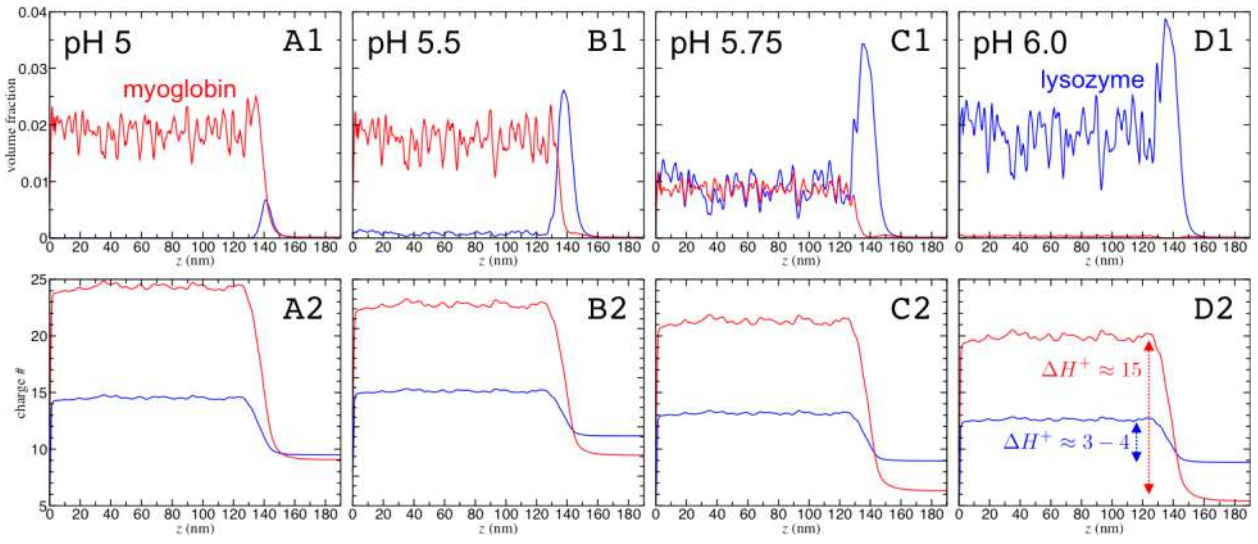

Figure 6. Top panels show the position-dependent volume fractions of both proteins at different pH, while bottom panels show protein local net charge number at the same conditions. ΔH^+ is the number of protons gained upon adsorption; [salt] = 1 mM and [myo] = [lyso] = 10 μM.

DOI: 10.1021/acs.macromol.8b01876
Macromolecules 2018, 51, 8205–8216

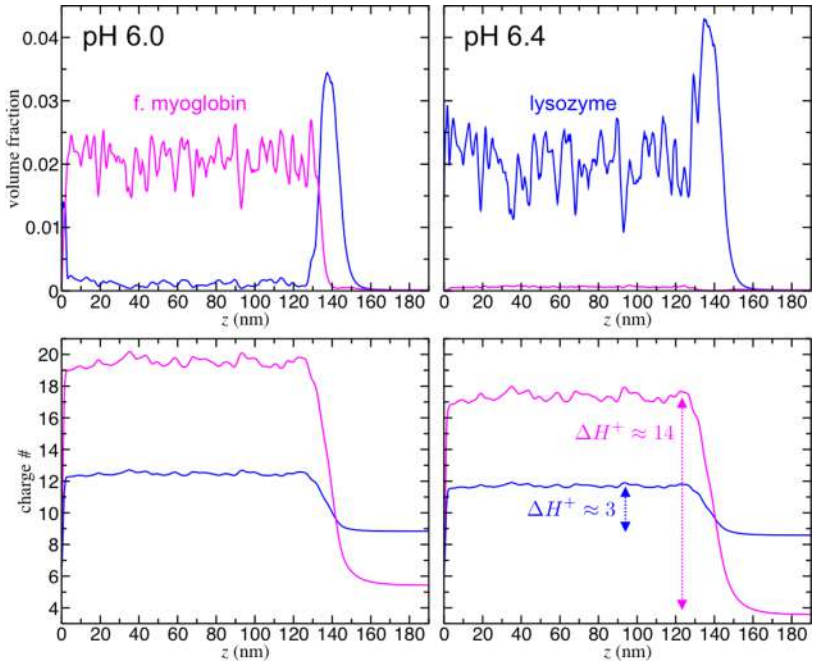

Figure 8. Top panels display the local volume fraction of both proteins for f. myoglobin−lysozyme mixtures at different pH, while bottom panels show protein local net charge at the same conditions. ΔH^+ is the number of protons gained upon adsorption; the concentration of both proteins is 10 μM and [salt] = 1 mM.

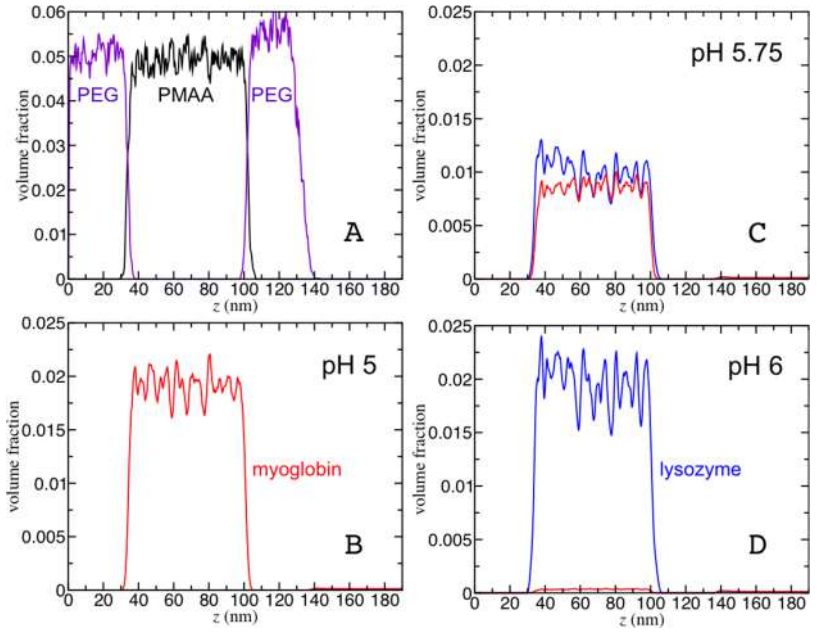

Figure 9. Plot of polymer (A) and protein (B) volume fraction as a function of the distance to the supporting surface for a PEG−PMAA−PEG network in contact with a myoglobin−lysozyme solution at pH 5. Panels C and D present local protein volume fractions for the same system at different solution pH. The concentration of both proteins is 10 μM and [salt] = 1 mM.

lead to the release of up to half of the total number of sodium ions inside the film (see the Supporting Information). This result indicates that counterion release from the network is an important contribution to protein adsorption at 1 mM salt.

In the following, we describe the molecular origin of the adsorption behavior observed in Figure 3, focusing on the low salt concentration conditions of panel A. Figure 4 depicts the volume fractions of both proteins and that of the polymer as a function of the distance from the supporting surface at bulk pH 2.5. In these z-dependent profiles, the adsorption behavior can be described through separating space in three clearly distinct regions. The polymer network extends up to 140 nm from the supporting surface. Under these conditions, there is no adsorption inside the film as the volume fraction of both proteins is negligible within this region (z < 140 nm). Far from the supporting surface (z > 160 nm), the volume fraction of each protein is that corresponding to the bulk solution. Bulk volume fractions are slightly different when comparing both proteins because they have different volumes, myoglobin being larger than lysozyme. Both proteins adsorb to the top surface

DOI: 10.1021/acs.macromol.8b01876
Macromolecules 2018, 51, 8205−8216

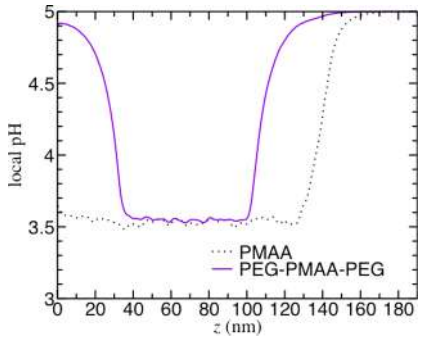

Figure 10. Local pH as a function of distance to the supporting surface for a PEG−PMAA−PEG (solid-line curve) and a PMAA (dotted-line curve) network in contact with a binary myoglobin−lysozyme solution with bulk pH 5. The concentration of both proteins is 10 μM and [salt] = 1 mM.

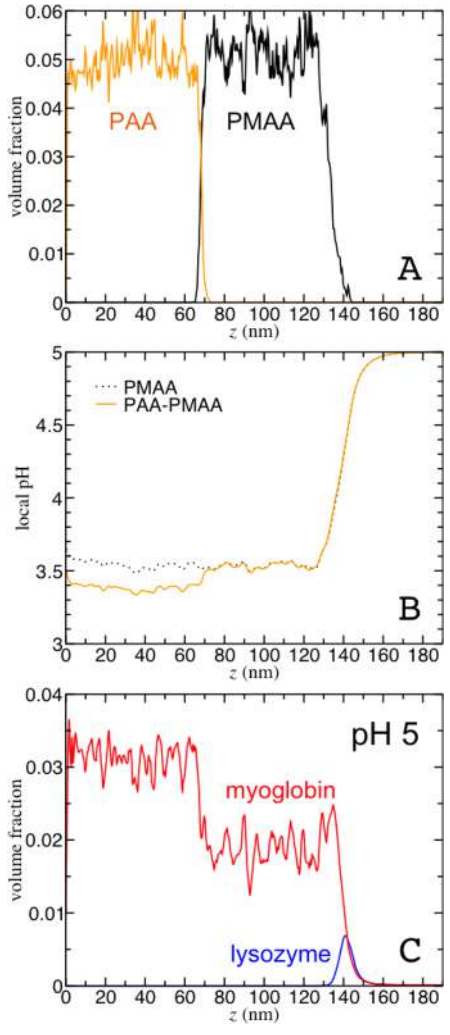

Figure 11. Plot of polymer (A) and protein (C) volume fraction as well as local pH (B) as a function of the distance to the supporting surface for a PAA−PMAA network in contact with a myoglobin−lysozyme solution at pH 5. Panel B also includes the local pH for pure PMAA network under the same conditions. The concentration of both proteins is 10 μM and [salt] = 1 mM.

of the film, which represents the interface between the solution (with bulk properties) and the hydrogel. This interfacial region extends for roughly 20 nm in the example shown in Figure 4. Here, we note that due to the geometry of the polymer network, its thickness is not very sensitive to pH changes.

Inside a polyacid network, pH drops with respect to the bulk solution.[49] When a molecule with titratable units adsorbs, this change in local pH results in charge regulation.[14] As a result, the net charge of the adsorbate is different inside and outside the polymer. Having both acidic and basic units with a variety of different pK_a's, proteins have many degrees of freedom to regulate their net charge under different conditions.[16] Inside a polyacid film the different amino acids of a protein display a higher degree of protonation which favors network−protein electrostatic attractions and enhances adsorption. At the same time, adsorption can modify the pH inside the film. The local pH is the result of the complex interplay between all of the physicochemical contributions to the thermodynamic potential, which results in equilibrium. For example, when a protein adsorbs, a lower local pH would result in a more positive net protein charge, which could enhance electrostatic attractions with the polymer network. Such lower pH, however, would induce protonation of MAA segments, leading to weaker polymer−protein attractions. In this context, local pH is an interesting quantity because it gives information about the local state of protonation of all species. To illustrate this behavior, Figure 5 shows the local pH for the polymer film in contact with a binary protein solution with bulk pH 5. The graph also shows the same quantity for a salt solution without proteins at the same conditions.

Three spatial regions can be seen in Figure 5. Relatively far from the supporting surface, the pH is that externally imposed to the bulk solution. Inside the film a lower pH than the bulk is established, which implies that proteins are more positively charged when adsorbed (see Figure 2). The presence of proteins in the solution increases the film pH with respect to the salt solution without the macromolecules. This implies that the polymer network is more negatively charged for protein solutions.

Figure 6 describes the behavior of myoglobin−lysozyme solutions in the pH region of highly competitive adsorption, where the transition occurs from adsorption of pure myoglobin (pH $\lesssim$ 5; see Figure 3A) to that of pure lysozyme (pH $\gtrsim$ 6). The graphs show the local volume fraction (upper panels) and net electric charge number (bottom panels) of both proteins. Mathematical expressions for these two quantities are provided in the Supporting Information. A clear feature of Figure 6, which is also observed in Figure 4, is that lysozyme adsorbs preferentially to the film−solution interface under most conditions. This prediction is consistent with the findings of Johansson et al.[57,58] showing that upon exposure to a lysozyme solution poly(acrylic acid) microgels display considerable higher protein concentration in the outer part of the network.

At pH $\lesssim$ 5 only myoglobin is found inside the film ($z \lesssim 140$ nm) in Figure 6. While the charge of both proteins is similar in the solution ($z \gtrsim 160$ nm), myoglobin is significantly more charged inside the polymer. This charge regulation is the result of a lower pH inside the film as seen in Figure 5.

When the bulk pH is 5.5, myoglobin still adsorbs preferentially inside the film, but we also see significant lysozyme adsorption to the upper film surface. This occurs because in the bulk solution (and the interface) lysozyme bears two more positive charges than myoglobin, the latter being more positively charged inside the film. At pH 5.75, both proteins roughly occupy the same volume inside the film. The intersection between the adsorption curves of myoglobin and

DOI: 10.1021/acs.macromol.8b01876
Macromolecules 2018, 51, 8205−8216

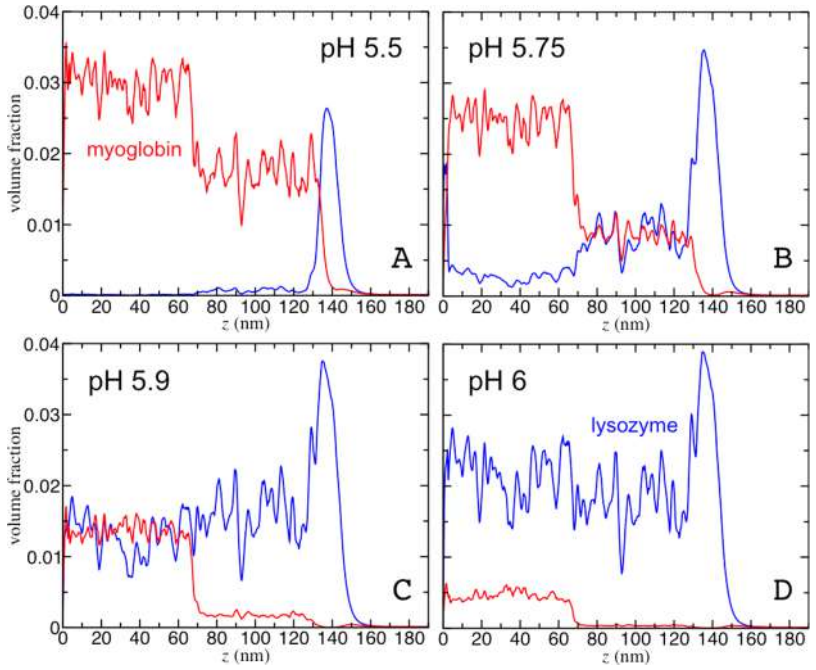

Figure 12. Plot of local protein volume fractions as a function of the distance to the supporting surface for a PAA−PMAA network in contact with a myoglobin−lysozyme solution at different pH. The concentration of both proteins is 10 μM and [salt] = 1 mM.

lysozyme occurs approximately at this bulk pH (see Figure 3A). Lysozyme, being significantly more charged outside the film, occupies the film−solution interface as well. This equipartition of the proteins inside the polymer is intriguing because myoglobin brings a net excess of ∼8 more positive charges to the film. Such behavior accentuates at pH 6, where myoglobin is still much more charged inside the film, but lysozyme adsorbs almost exclusively.

Why does the more weakly charged lysozyme adsorb instead of myoglobin under some conditions in Figure 6? This behavior cannot be the consequence of their charge distribution, lysozyme potentially capable of better orientating its positive charges to favor adsorption. Such a phenomenon can only contribute significantly to adsorption in the interface between the polymer and the solution. Inside the film negative charges are distributed in three dimensions, and any protein orientation will also expose it to protein−network electrostatic repulsions. One possibility to explain this adsorption behavior is the free energy cost of protonation. At a given bulk pH, the chemical free energy that describes acid−base equilibrium of an amino acid is minimal when the degree of protonation is that of the bulk. Namely, when a protein adsorbs, protonation due to the lower pH inside the film results in an increase of the chemical free energy. This cost of protonation upon adsorption is under many different conditions, outweighed by the decrease in electrostatic energy resulting from the polymer−protein attractions. At pH 6, for example, lysozyme gains 3−4 protons upon adsorption inside the film, while myoglobin would need to protonate 15 times. Thus, the chemical free energy cost of adsorbing lysozyme is significantly smaller.

The other possibility to explain the behavior described in Figure 6 is the different size of the proteins. Adsorption of the weaker-charged lysozyme, being smaller than myoglobin, can potentially result in more density of positive charge at the same entropic cost of macromolecular confinement. To determine whether the adsorption of the more weakly charged protein results from the size of the proteins or the cost of protonation, we have designed a fictitious myoglobin where the volume of each amino acid has been rescaled so that the total volume of the molecule is identical to that of lysozyme. The structure and sequence of this toy protein are the same as those of myoglobin, taken from crystallographic data.

Figure 7 shows the pH-dependent adsorption from binary solutions of lysozyme and fictitious myoglobin. When comparing this adsorption to that of actual myoglobin in binary mixtures, we see that protein size does indeed play a significant role: The film adsorbs considerably more of the smaller (fictitious) myoglobin and in a larger range of pH. In addition, the adsorption of lysozyme is displaced to higher pH values.

Figure 8 shows the position-dependent volume fraction of lysozyme and fictitious myoglobin in binary mixtures corresponding to some of the conditions shown in Figure 7. At pH 6, the film adsorbs the toy protein, which is the more charged one (inside the film), as opposed to the pure lysozyme adsorption seen in Figure 6 for binary mixtures including actual myoglobin. At a slightly larger pH of 6.4, however, the same phenomenon occurs as in the myoglobin−lysozyme solution; the film preferentially absorbs the more weakly charged protein. Now, because both proteins have the same size, this phenomenon can only be attributed to the cost of protonation. Upon adsorption at pH 6.4, lysozyme gains ∼3 protons, while fictitious myoglobin gains 14, which carries a much higher cost of protonation.

As the adsorption curves of Figure 3 show, the system's pH can be used to switch from the adsorption of one to the other protein. Furthermore, the local volume fraction profiles of Figure 6 show that a different protein can be predominantly found at different spatial regions of the system (myoglobin inside the film and lysozyme on the top surface) at the same experimental conditions. This behavior points to the possibility of designing the molecular composition of the polymer network to achieve protein separation and/or localization using the solution pH. Using the following results, we address

DOI: 10.1021/acs.macromol.8b01876
Macromolecules 2018, 51, 8205−8216

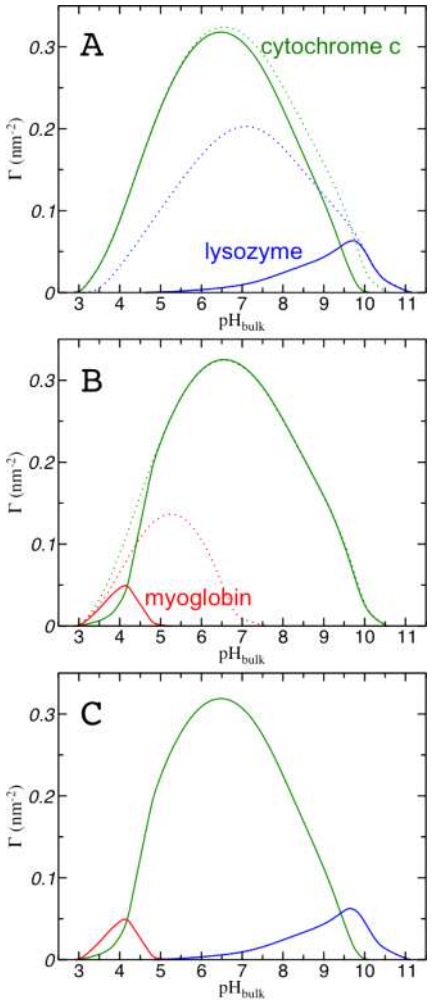

Figure 13. Adsorption from binary lysozyme−cytochrome *c* (A) and myoglobin−cytochrome *c* (B) solutions to a PMAA film as a function of solution pH. In these panels, dotted-line curves represent the adsorption from single protein solutions. Panel C shows the adsorption from a mixture of the three proteins. In all cases, the concentration of each proteins is 10 μM and [salt] = 1 mM.

two questions: (i) Is it possible to control the position and thickness of the film's spatial region where the proteins adsorb? (ii) Is it feasible to adsorb two different proteins in two different regions (not only at the top surface but) inside the film?

To answer the first question, we design a hydrogel film where the ionizable PMAA chains occupy the middle portion of the network, while the bottom and top regions of the network are composed of electroneutral poly(ethylene glycol) (PEG) chains. This polymer is currently used in various biomaterial applications due to its hydrophilicity, biocompatibility, and antifouling properties.[59−61] In Figure 9, we describe protein adsorption from a binary myoglobin−lysozyme solution to such a PEG−PMAA−PEG network.

Figure 9A illustrates the position-dependent local volume faction of both methacrylic acid and ethylene glycol network segments at pH 5. MAA segments are indeed only found in the intermediate region of the network (40 nm $\lesssim z \lesssim$ 100 nm), while PEG segments are found at both the bottom (0 < $z \lesssim$ 40 nm) and the upper (100 nm $\lesssim z \lesssim$ 140 nm) regions of the network. Under these conditions, only myoglobin adsorbs as seen in Figure 9B. Similarly to the behavior observed for the pure PMAA network, increasing pH to 5.75 results in the presence of a mixture of both proteins inside the film (Figure 9C), while further increasing pH to 6 leads to the adsorption of only lysozyme (Figure 9D). However, in all these cases adsorption is confined to the intermediate region of the film where MAA is present. Panels B−D of Figure 9 show that almost no protein partitions to the PEG region. The presence of the electroneutral polymer also prevents the accumulation of lysozyme on the top surface of the ionizable layer observed for a pure PMAA network (see Figure 6).

Another way of understanding this localization of proteins is through the local pH. Figure 10 shows the drop in pH inside the polymer film for the PEG−PMAA−PEG network and the (pure) PMAA network under the same conditions. In both structures, local pH is approximately the same in the region where PMAA is present, which together with the fact that the local density of ionizable polymer is similar in such region (see Figures 4B and 9A) results in the partition of approximately the same local amount of lysozyme in this region (compare Figures 6A1 and 9B). However, such lower pH, which allows for the proteins to regulate charge and adsorb, occurs in a narrower spatial region consistent with the region occupied by PMAA. In the regions that PEG occupies, next to the surface and near the film−solution interface, local pH approaches the bulk value.

The pH range of highly competitive adsorption is narrow (although 1 pH unit is a 10-fold increase in proton concentration). In Figure 6, we see that the transition between pure myoglobin to pure lysozyme adsorption occurs in less than a pH unit. To profit from this behavior, we design a network composed of two polymers with slightly different acid dissociation constants. This network is composed of two layers where the upper portion is made of PMAA chains while poly(acrylic acid) (PAA) chains occupy the lower region (with pK_a = 4.65 and 4.25, respectively).

Figure 11 illustrates the behavior of the PAA−PMAA film in contact with a myoglobin−lysozyme solution at pH and 1 mM salt concentration. Panel A presents the local polymer volume fraction to show that indeed PAA occupies the lower region of the film (0 < $z \lesssim$ 70 nm) while PMAA is present in the film's upper region (70 nm $\lesssim z \lesssim$ 140 nm). This polymer distribution results in a slight drop in pH in the region of PAA, respect to a pure PMAA network, which can be observed in panel B of Figure 11. This small drop, however, has a significant influence on the partition of myoglobin inside the film. Panel C shows that the local volume fraction of this protein is significantly larger in the region of PAA due to the lower pH (or equivalently the higher density of deprotonated, negatively charged polymer segments).

Figure 12 shows the volume fractions of myoglobin and lysozyme for a binary solution in equilibrium with a PAA−PMAA film. Similarly to the behavior reported for the PMAA film, the network with two acidic units transitions from the adsorption of pure myoglobin to almost exclusively lysozyme as pH is varied from 5 to 6 (see Figures 11C and 12D). However, when considering the region of highly competitive adsorption, a much richer behavior emerges for the PAA−PMAA film. In Figure 12, it is possible to clearly see different spatial distribution of proteins depending on the solution pH: (i) only myoglobin inside the network and lysozyme adsorbed at the top surface (panel A with pH 5.5), (ii) myoglobin in the lower region (PAA) and a mixture in the upper region (PMAA) with lysozyme at the interface (panel B with pH

DOI: 10.1021/acs.macromol.8b01876
Macromolecules 2018, 51, 8205−8216

5.75), and (iii) a mixture in the lower region and only lysozyme in the upper region and the interface (panel C with pH 5.9).

Finally in Figure 13, we consider binary and ternary protein solutions containing cytochrome *c*. Comparing the adsorption of single-protein solutions to the results for binary and ternary solutions reveals that adsorption of cytochrome *c* is only slightly influenced by the presence of either lysozyme or myoglobin or both. In these mixtures adsorption of cytochrome *c* is predominant in a wide range of pH values. In contrast, adsorption of myoglobin as well as that of lysozyme is significantly affected by to the presence of cytochrome *c*. Cytochrome *c* completely prevents the adsorption of myoglobin at higher pH and that of lysozyme at lower pH. At the same time the magnitude of the adsorption decreases by more than a half for both proteins.

DISCUSSION AND CONCLUSION

In this work, we present theoretical predictions for the equilibrium adsorption from binary and ternary mixtures of myoglobin, lysozyme, and cytochrome *c* to pH-responsive hydrogel films. These are three globular proteins of similar size typically considered in case studies. The theory that we have used in this study allows for a molecular-level description of all the components of the system incorporating size, shape, charge distribution, and conformational degrees of freedom of all species. In this method the protonation state of a molecule is predicted at each position as a result of the local environment and the interplay between all the physicochemical contributions to the free energy.

When these proteins are in solution, decreasing the salt concentration significantly enhances their adsorption to the film. This is because of the screening effect of salt ions and their critical role in regulating the extent of network−protein electrostatic interactions. We have focused our attention in relatively low salt concentration solutions where significant protein adsorption can be achieved. Under such conditions, local pH drops inside PMAA films, which leads to an increased protonation of proteins inside the film, enhancing the electrostatic attractions with the polymer that drive the adsorption.

In the absence of proteins the drop in pH inside the film occurs to reduce network segment electrostatic repulsions. Even at the low protein concentrations (10 μM) of this work, we observe that the pH inside the film is slightly higher upon adsorption (with respect to solutions without proteins). Such increase in film pH allows the network to become more negatively charged, which favors electrostatic attractions and decreases the chemical free energy that describes the acid−base equilibrium of the PMAA units. However, if pH increases further, the adsorbed proteins become less positively charged and the electrostatic attractions weaken. Thus, the pH that establishes inside the film represents the balance between these different contributions that drive opposite behaviors. In this context, local pH is a useful quantity because it is a single quantity that simultaneously provide information about the state of charge of all species in the vicinity.

We have concentrated our attention in myoglobin−lysozyme mixtures, where selective adsorption of one or the other protein can be achieved through changing the solution pH. At low (but sufficiently high) pH only myoglobin is present inside the film, while lysozyme is the only species that adsorbs at intermediate and high pH. In these binary mixtures, competitive adsorption is a fair game only in a narrow range of pH (under the conditions of this present study); the transition between pure myoglobin to pure lysozyme adsorption occurs in one unit of pH between 5 and 6. Depending on the pH within this range, the system displays distinctive features: (i) the adsorption of different proteins inside the film and at the top surface or (ii) the adsorption of a mixture of proteins inside the film.

This pH-controlled spatial distribution of proteins suggested the possibility of using network chemical composition to further separate/localize the proteins. Through sandwiching a relatively thin layer of PMAA with layers of a neutral polymer, one can precisely confine the protein within the thin ionizable layer. The volume fraction of either protein is almost zero in the neutral regions of the film as there are no electrostatic attractions that outweight the entropic cost of confinement inside the film. In addition, the structure of this network allows for controlling the spatial region where the pH drops, which defines local state of protonation.

Moreover, a network structure composed of two layers of different polyacid chains can be used to create an additional drop in the local pH inside the film. We have considered acids with similar pK_a: MAA and AA. Similar to the pure PMAA film, this two-layer film is suitable for protein separation displaying pure adsorption of either myoglobin at low pH or lysozyme for neutral and alkaline solutions. In the transition range of pH, however, the adsorption behavior in the two-layer structure becomes richer than in the PMAA film; using the solution pH, it is possible to control which protein adsorbs to each layer of the PAA−PMAA network.

The size of the protein and its net charge in the lower pH environment inside the film play an important role in the adsorption behavior. However, the chemical free energy cost of protonation plays a critical role in determining which protein adsorbs in binary and ternary mixtures. For example, under the conditions studied in this work, only lysozyme adsorbs around and above pH 6 in binary mixtures with myoglobin, though this latter protein would be significantly more positively charged inside the film. As opposed to incorporating lysozyme, the adsorption of myoglobin under such conditions would require the gain of an order of magnitude more protons. In binary and ternary mixtures containing cytochrome *c*, selective adsorption of one or the other protein upon changing the system's pH can still be observed; however, cytochrome *c* significantly reduces the pH range and the amount of myoglobin and lysozyme adsorption. Cytochrome *c* is the smallest of the three proteins, and its adsorption requires a similar degree of protonation as lysozyme.

In summary, we have described some of the key features of the physical chemistry that underlies protein adsorption to pH-responsive hydrogel films. These films and the pH gradients they induce can serve for the separation of proteins from mixtures and their localization with nanometer resolution. In this work, we have focused on competitive protein adsorption due to electrostatic attractions and have not evaluated the possibility of protein−network hydrogen bond formation. This effect may contribute to protein adsorption in the low pH range (<3), where the polymer network is weakly charged. We will investigate this phenomenon in future work and consider the effect of temperature on protein adsorption. Finally, the method we have developed is completely general and can be employed to study a variety of problems involving molecular adsorption to polymer films. Indeed, we are currently

DOI: 10.1021/acs.macromol.8b01876
Macromolecules 2018, 51, 8205−8216

investigating the use of polybase hydrogel films for the sequestration and removal of pesticides.

■ ASSOCIATED CONTENT

Supporting Information

The Supporting Information is available free of charge on the ACS Publications website at DOI: 10.1021/acs.macromol.8b01876.

Full description of the theoretical method; additional results (PDF)

■ AUTHOR INFORMATION

Corresponding Author

*E-mail: longogs@inifta.unlp.edu.ar (G.S.L.).

ORCID

Gabriel S. Longo: 0000-0001-8353-5163

Notes

The authors declare no competing financial interest.

■ ACKNOWLEDGMENTS

This work was supported by CONICET and ANPCyT (PICT-2014-3377), Argentina.

■ REFERENCES

(1) Koetting, M. C.; Peppas, N. A. pH-responsive poly(itaconic acid-co-N-vinylpyrrolidone) hydrogels with reduced ionic strength loading solutions offer improved oral delivery potential for high isoelectric point-exhibiting therapeutic proteins. *Int. J. Pharm.* **2014**, *471*, 83−91.

(2) Asayama, W.; Sawada, S.; Taguchi, H.; Akiyoshi, K. Comparison of refolding activities between nanogel artificial chaperone and GroEL systems. *Int. J. Biol. Macromol.* **2008**, *42*, 241−246.

(3) Sawada, S. I.; Akiyoshi, K. Nano-encapsulation of lipase by self-assembled nanogels: Induction of high enzyme activity and thermal stabilization. *Macromol. Biosci.* **2010**, *10*, 353−358.

(4) Vermonden, T.; Censi, R.; Hennink, W. E. Hydrogels for protein delivery. *Chem. Rev.* **2012**, *112*, 2853−2888.

(5) Peppas, N. A.; Hilt, J. Z.; Khademhosseini, A.; Langer, R. Hydrogels in biology and medicine: From molecular principles to bionanotechnology. *Adv. Mater.* **2006**, *18*, 1345−1360.

(6) Hoffman, A. S. Stimuli-responsive polymers: Biomedical applications and challenges for clinical translation. *Adv. Drug Delivery Rev.* **2013**, *65*, 10−16.

(7) Matricardi, P.; Di Meo, C.; Coviello, T.; Hennink, W. E.; Alhaique, F. Interpenetrating polymer networks polysaccharide hydrogels for drug delivery and tissue engineering. *Adv. Drug Delivery Rev.* **2013**, *65*, 1172−1187.

(8) Zhang, X.; Guan, Y.; Zhang, Y. Ultrathin hydrogel films for rapid optical biosensing. *Biomacromolecules* **2012**, *13*, 92−97.

(9) Islam, M. R.; Gao, Y.; Li, X.; Serpe, M. J. Responsive polymers for biosensing and protein delivery. *J. Mater. Chem. B* **2014**, *2*, 2444−2451.

(10) Wu, W.; Mitra, N.; Yan, E. C. Y.; Zhou, S. Multifunctional Hybrid Nanogel for and Self-Regulated Insulin Release at Physiological pH. *ACS Nano* **2010**, *4*, 4831−4839.

(11) Luensmann, D.; Jones, L. Protein deposition on contact lenses: The past, the present, and the future. *Contact Lens Anterior Eye* **2012**, *35*, 53−64.

(12) Omali, N. B.; Subbaraman, L. N.; Coles-Brennan, C.; Fadli, Z.; Jones, L. W. Biological and clinical implications of lysozyme deposition on soft contact lenses. *Optom. Vis. Sci.* **2015**, *92*, 750−757.

(13) Green, R. J.; Davies, M. C.; Roberts, C. J.; Tendler, S. J. B. Competitive protein adsorption as observed by surface plasmon resonance. *Biomaterials* **1999**, *20*, 385−391.

(14) Longo, G. S.; Olvera de la Cruz, M.; Szleifer, I. Equilibrium adsorption of hexahistidine on pH-responsive hydrogel nanofilms. *Langmuir* **2014**, *30*, 15335−15344.

(15) Narambuena, C. F.; Longo, G. S.; Szleifer, I. Lysozyme adsorption in pH-responsive hydrogel thin-films: The non-trivial role of acid-base equilibrium. *Soft Matter* **2015**, *11*, 6669−6679.

(16) Longo, G. S.; Szleifer, I. Adsorption and protonation of peptides and proteins in pH responsive gels. *J. Phys. D: Appl. Phys.* **2016**, *49*, 323001.

(17) Welsch, N.; Becker, A. L.; Dzubiella, J.; Ballauff, M. Core-shell microgels as smart carriers for enzymes. *Soft Matter* **2012**, *8*, 1428−1436.

(18) Zhang, Z.; Zhang, R.; Zou, L.; McClements, D. J. Protein encapsulation in alginate hydrogel beads: Effect of pH on microgel stability, protein retention and protein release. *Food Hydrocolloids* **2016**, *58*, 308−315.

(19) Lassen, B.; Malmsten, M. Competitive protein adsorption at plasma polymer surfaces. *J. Colloid Interface Sci.* **1997**, *186*, 9−16.

(20) Ying, P.; Yu, Y.; Jin, G.; Tao, Z. Competitive protein adsorption studied with atomic force microscopy and imaging ellipsometry. *Colloids Surf., B* **2003**, *32*, 1−10.

(21) Li, S.; Mulloor, J. J.; Wang, L.; Ji, Y.; Mulloor, C. J.; Micic, M.; Orbulescu, J.; Leblanc, R. M. Strong and selective adsorption of lysozyme on graphene oxide. *ACS Appl. Mater. Interfaces* **2014**, *6*, 5704−5712.

(22) Moerz, S. T.; Huber, P. pH-dependent selective protein adsorption into mesoporous silica. *J. Phys. Chem. C* **2015**, *119*, 27072−27079.

(23) Saxena, A.; Kumar, M.; Tripathi, B. P.; Shahi, V. K. Organic-inorganic hybrid charged membranes for proteins separation: Isoelectric separation of proteins under coupled driving forces. *Sep. Purif. Technol.* **2010**, *70*, 280−290.

(24) Kubiak-Ossowska, K.; Mulheran, P. A. Mechanism of hen egg white lysozyme adsorption on a charged solid surface. *Langmuir* **2010**, *26*, 15954−15965.

(25) Wei, T.; Carignano, M. A.; Szleifer, I. Lysozyme adsorption on polyethylene surfaces: Why are long simulations needed? *Langmuir* **2011**, *27*, 12074−12081.

(26) Li, R.; Chen, R.; Chen, P.; Wen, Y.; Ke, P. C.; Cho, S. S. Computational and experimental characterizations of silver nanoparticle-apolipoprotein biocorona. *J. Phys. Chem. B* **2013**, *117*, 13451−13456.

(27) Ding, F.; Radic, S.; Chen, R.; Chen, P.; Geitner, N. K.; Brown, J. M.; Ke, P. C. Direct observation of a single nanoparticle-ubiquitin corona formation. *Nanoscale* **2013**, *5*, 9162−9169.

(28) Ding, H.-m.; Ma, Y.-q. Computer simulation of the role of protein corona in cellular delivery of nanoparticles. *Biomaterials* **2014**, *35*, 8703−8710.

(29) Shao, Q.; Hall, C. K. Protein adsorption on nanoparticles: Model development using computer simulation. *J. Phys.: Condens. Matter* **2016**, *28*, 414019.

(30) Tavanti, F.; Pedone, A.; Menziani, M. C. Competitive binding of proteins to gold nanoparticles disclosed by molecular dynamics simulations. *J. Phys. Chem. C* **2015**, *119*, 22172−22180.

(31) Torres, P.; Bojanich, L.; Sanchez-Varretti, F.; Ramirez-Pastor, A. J.; Quiroga, E.; Boeris, V.; Narambuena, C. F. Protonation of β-lactoglobulin in the presence of strong polyelectrolyte chains: A study using Monte Carlo simulation. *Colloids Surf., B* **2017**, *160*, 161−168.

(32) Sofronova, A. A.; Evstafyeva, D. B.; Izumrudov, V. A.; Muronetz, V. I.; Semenyuk, P. I. Protein-polyelectrolyte complexes: Molecular dynamics simulations and experimental study. *Polymer* **2017**, *113*, 39−45.

(33) Yigit, C.; Welsch, N.; Ballauff, M.; Dzubiella, J. Protein sorption to charged microgels: characterizing binding isotherms and driving forces. *Langmuir* **2012**, *28*, 14373−14385.

(34) Angioletti-Uberti, S.; Ballauff, M.; Dzubiella, J. Dynamic density functional theory of protein adsorption on polymer-coated nanoparticles. *Soft Matter* **2014**, *10*, 7932−7945.

DOI: 10.1021/acs.macromol.8b01876
Macromolecules 2018, 51, 8205−8216

(35) Sun, T.-Y.; Liang, L.-J.; Wang, Q.; Laaksonen, A.; Wu, T. A molecular dynamics study on pH response of protein adsorbed on peptide-modified polyvinyl alcohol hydrogel. *Biomater. Sci.* **2014**, *2*, 419−426.
(36) Szleifer, I. Protein adsorption on surfaces with grafted polymers. *Biophys. J.* **1997**, *72*, 595−612.
(37) Fang, F.; Satulovsky, J.; Szleifer, I. Kinetics of protein adsorption and desorption on surfaces with grafted polymers. *Biophys. J.* **2005**, *89*, 1516−1533.
(38) Oberle, M.; Yigit, C.; Angioletti-Uberti, S.; Dzubiella, J.; Ballauff, M. Competitive protein adsorption to soft polymeric layers: binary mixtures and comparison to theory. *J. Phys. Chem. B* **2015**, *119*, 3250−3258.
(39) Nap, R.; Gong, P.; Szleifer, I. Weak polyelectrolytes tethered to surfaces: Effect of geometry, acid-base equilibrium and electrical permittivity. *J. Polym. Sci., Part B: Polym. Phys.* **2006**, *44*, 2638−2662.
(40) Gong, P.; Genzer, J.; Szleifer, I. Phase behavior and charge regulation of weak polyelectrolyte grafted layers. *Phys. Rev. Lett.* **2007**, *98*, 018302.
(41) Mann, B. A.; Holm, C.; Kremer, K. Swelling of polyelectrolyte networks. *J. Chem. Phys.* **2005**, *122*, 154903.
(42) Quesada-Pérez, M.; Maroto-Centeno, J. A.; Martín-Molina, A. Effect of the counterion valence on the behavior of thermo-sensitive gels and microgels: A Monte Carlo simulation study. *Macromolecules* **2012**, *45*, 8872−8879.
(43) Košovan, P.; Richter, T.; Holm, C. Modeling of polyelectrolyte gels in equilibrium with salt solutions. *Macromolecules* **2015**, *48*, 7698−7708.
(44) Hofzumahaus, C.; Hebbeker, P.; Schneider, S. Monte Carlo simulations of weak polyelectrolyte microgels: pH-dependence of conformation and ionization. *Soft Matter* **2018**, *14*, 4087−4100.
(45) Berendsen, H. J. C.; van der Spoel, D.; van Drunen, R. GROMACS: A message-passing parallel molecular dynamics implementation. *Comput. Phys. Commun.* **1995**, *91*, 43−56.
(46) van der Spoel, D.; Lindahl, E.; Hess, B.; Groenhof, G.; Mark, A. E.; Berendsen, H. J. C. GROMACS: Fast, flexible, and free. *J. Comput. Chem.* **2005**, *26*, 1701−1718.
(47) Abraham, M. J.; Murtola, T.; Schulz, R.; Páll, S.; Smith, J. C.; Hess, B.; Lindahl, E. GROMACS: High performance molecular simulations through multi-level parallelism from laptops to supercomputers. *SoftwareX* **2015**, *1−2*, 19−25.
(48) Kremer, K.; Grest, G. S. Dynamics of entangled linear polymer melts: A molecular-dynamics simulation. *J. Chem. Phys.* **1990**, *92*, 5057−5086.
(49) Longo, G. S.; Olvera de la Cruz, M.; Szleifer, I. Molecular theory of weak polyelectrolyte gels: The role of pH and salt concentration. *Macromolecules* **2011**, *44*, 147−158.
(50) Grimsley, G. R.; Scholtz, J. M.; Pace, C. N. A summary of the measured pK values of the ionizable groups in folded proteins. *Protein Sci.* **2008**, *18*, 247−251.
(51) Teixeira, A. A. R.; Lund, M.; Barroso da Silva, F. L. Fast proton titration scheme for multiscale modeling of protein solutions. *J. Chem. Theory Comput.* **2010**, *6*, 3259−3266.
(52) Hubbard, S. R.; Hendrickson, W. A.; Lambright, D. G.; Boxer, S. G. X-ray crystal structure of a recombinant human myoglobin mutant at 2.8 Å resolution. *J. Mol. Biol.* **1990**, *213*, 215−218.
(53) Vaney, M. C.; Maignan, S.; Riès-Kautt, M.; Ducruix, A. High-resolution structure (1.33 Å) of a HEW lysozyme tetragonal crystal grown in the APCF apparatus. Data and structural comparison with a crystal grown under microgravity from SpaceHab-01 mission. *Acta Crystallogr., Sect. D: Biol. Crystallogr.* **1996**, *52*, 505−517.
(54) Mirkin, N.; Jaconcic, J.; Stojanoff, V.; Moreno, A. High resolution X-ray crystallographic structure of bovine heart cytochrome c and its application to the design of an electron transfer biosensor. *Proteins: Struct., Funct., Genet.* **2008**, *70*, 83−92.
(55) Becker, A. L.; Henzler, K.; Welsch, N.; Ballauff, M.; Borisov, O. Proteins and polyelectrolytes: A charged relationship. *Curr. Opin. Colloid Interface Sci.* **2012**, *17*, 90−96.
(56) Moerz, S. T.; Huber, P. Protein adsorption into mesopores: A combination of electrostatic interaction, counterion release, and van der Waals forces. *Langmuir* **2014**, *30*, 2729−2737.
(57) Johansson, C.; Hansson, P.; Malmsten, M. Interaction between lysozyme and poly(acrylic acid) microgels. *J. Colloid Interface Sci.* **2007**, *316*, 350−359.
(58) Johansson, C.; Hansson, P.; Malmsten, M. Mechanism of lysozyme uptake in poly(acrylic acid) microgels. *J. Phys. Chem. B* **2009**, *113*, 6183−6193.
(59) Hucknall, A.; Rangarajan, S.; Chilkoti, A. In pursuit of zero: Polymer brushes that resist the adsorption of proteins. *Adv. Mater.* **2009**, *21*, 2441−2446.
(60) Rodriguez Emmenegger, C.; Brynda, E.; Riedel, T.; Sedlakova, Z.; Houska, M.; Alles, A. B. Interaction of blood plasma with antifouling surfaces. *Langmuir* **2009**, *25*, 6328−6333.
(61) Riedel, T.; Riedelová-Reicheltová, Z.; Májek, P.; Rodriguez-Emmenegger, C.; Houska, M.; Dyr, J. E.; Brynda, E. Complete identification of proteins responsible for human blood plasma fouling on poly(ethylene glycol)-based surfaces. *Langmuir* **2013**, *29*, 3388−3397.

DOI: 10.1021/acs.macromol.8b01876
Macromolecules 2018, 51, 8205−8216